J Physiol 599.6 (2021) pp 1769–1782

The Journal of Physiology

SYMPOSIUM REVIEW

How does oxygen diffuse from capillaries to tissue mitochondria? Barriers and pathways

Sally C. Pias

Department of Chemistry, New Mexico Institute of Mining and Technology (New Mexico Tech), Socorro, NM, USA

Edited by: Laura Bennet & Satoshi Matsuoka

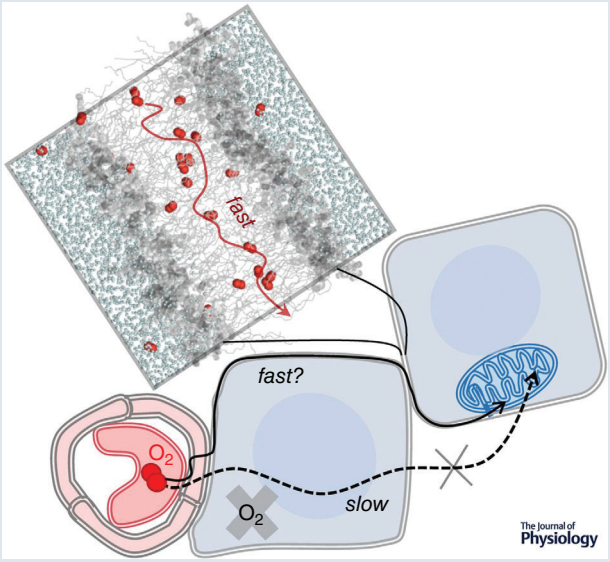

Abstract Timely delivery of oxygen (O_2) to tissue mitochondria is so essential that elaborate circulatory systems have evolved to minimize diffusion distances within tissue. Yet, knowledge is surprisingly limited regarding the diffusion pathway between blood capillaries and tissue mitochondria. An established and growing body of work examines the influence cellular and extracellular structures may have on subcellular oxygen availability. This brief review discusses the physiological and pathophysiological significance of oxygen availability, highlights recent computer modelling studies of transport at the cell-membrane level, and considers alternative diffusion pathways within tissue. Experimental and computer modelling studies suggest that oxygen diffusion may be accelerated by cellular lipids, relative to cytosolic and interstitial fluids.

Sally Pias is a computational chemist with doctoral training in biochemistry. She is currently an associate professor in the Department of Chemistry at the New Mexico Institute of Mining and Technology (New Mexico Tech). She has a long-standing interest in the physical mechanism of tissue-level oxygen delivery. Sally is actively involved in the Biophysical Society and its subgroup on Bioenergetics, Mitochondria, and Metabolism. She is also involved in the leadership of the International Society on Oxygen Transport to Tissue (ISOTT) and is a past recipient of ISOTT's Melvin H. Knisely Award.

This review expands upon a Featured Lecture, 'Computer modelling of oxygen transport in cells and tissues', presented at the 47th meeting of the International Society on Oxygen Transport to Tissue (ISOTT), held 28–31 July 2019 in Albuquerque, NM, USA.

DOI: 10.1113/JP278815

Such acceleration, or 'channelling', would occur due to greatly enhanced oxygen solubility in lipids, especially near the midplane of lipid bilayers. Rapid long-range movement would be promoted by anisotropically enhanced lateral diffusion of oxygen along the midplane and by junctions holding lipid structures in close proximity to one another throughout the tissue. Clarifying the biophysical mechanism of oxygen transport within tissue will shed light on limitations and opportunities in tumour radiotherapy and tissue engineering.

(Received 17 March 2020; accepted after revision 11 November 2020; first published online 20 November 2020)
Corresponding author S. C. Pias: Department of Chemistry, New Mexico Tech, 801 Leroy Place, Socorro, NM 87801, USA. Email: sally.pias@nmt.edu

Abstract figure legend The path of oxygen (O_2) diffusion after release from red blood cells is unknown, but oxygen has commonly been assumed to traverse cell bodies to reach mitochondria several cell layers beyond the capillary. This review examines potential diffusion pathways dominated by aqueous fluids (via cell bodies and interstitial fluid) or by lipids (via 'hydrophobic channelling' between the lipid leaflets of membranes). It considers evidence from experimental and theoretical studies, especially with regard to oxygen solubility and diffusion as well as permeability and resistance along aqueous and lipid-based pathways. The relative rate of oxygen movement along the potential pathways is considered, with the aim of discerning whether lipid-based pathways influence the rate of oxygen diffusional delivery within tissues.

Physiological implications of oxygen availability

The great physiological significance of oxygen (O_2) transport is highlighted by the awarding of the 2019 Nobel Prize in Physiology or Medicine to three researchers recognized for discoveries related to cells' response to oxygen availability. Hypoxia and related signalling effects have long been associated with cancer phenotype and aetiology (Elas *et al.* 2003; Vaupel and Mayer, 2007; Ruan *et al.* 2009). Even so, the oxygen tension measured in tumours can be highly dynamic and heterogeneous, with both temporal and spatial variations of P_{O_2} within a tumour (Elas *et al.* 2003; Vaupel and Mayer, 2007; Michiels *et al.* 2016). Tissue hypoxia tends to reduce the effectiveness of radiotherapy and of many drugs (Höckel *et al.* 1996; Vaupel and Mayer, 2007). Conversely, the therapeutic efficacy of radiation can be enhanced by up to three times under adequately oxygenated conditions, relative to profound hypoxia (Hall, 2006, cited in Hou *et al.* 2009). Numerous studies have shown that coordinating tumour oxygenation with radiotherapy timing and spatial application can enhance therapeutic outcomes (Höckel *et al.* 1996; Elas *et al.* 2003; Hou *et al.* 2009; Carreau *et al.* 2011; and others reviewed in Colliez *et al.* 2017). Therefore, identifying tissue structural and compositional parameters that modulate the availability of oxygen in tumour tissue – and within the cells of the tissue – may reveal strategies to improve tumour therapy outcomes.

The work reviewed here takes a physical–structural view of the tissue milieu. Although simplified models have treated oxygen diffusion within tissue as occurring in a homogeneous medium (Krogh, 1929, cited in Longmuir, 1981), tissue is now well-known to be inhomogeneous. The inhomogeneity may be exaggerated where cellular structural alterations occur. Such changes are particularly evident in cancers, where the level of organization of the microvasculature and the tissue tends to diminish, the fraction of interstitial fluid tends to increase, and certain cell types may become more abundant relative to others (Vaupel, 2004; Multhoff and Vaupel, 2012; Ding *et al.* 2019*a*). Moreover, the number of connections among cells in tumours may decrease (Cavallaro & Christofori, 2001). Associated changes in the physicochemical properties of the tissue may contribute to hypoxia and may help explain spatial heterogeneities in oxygen distribution.

Numerous pathologies other than cancer are affected by tissue-level oxygen availability, including diabetic peripheral hypoxia (Cicco *et al.* 2011) as well as ischaemic hypoxia and reperfusion injury surrounding stroke and traumatic brain injury (Kalogeris *et al.* 2016; Yokobori *et al.* 2018). Diffusive delivery becomes especially important under circumstances where vessels are occluded or sparsely distributed, or where convective oxygen delivery via red blood cells is compromised, as in sickle cell disease. Moreover, the problem of diffusive delivery is apparent in engineered tissue constructs. These are structured tissue mimics cultivated in the laboratory with applications in regenerative medicine, organ replacement and as model systems for investigating tissue function and disease (Volkmer *et al.* 2008; Jakab *et al.* 2010; Murphy *et al.* 2019). In engineered constructs, undifferentiated cells are often deposited within a structural support, such as a polymer matrix, followed by differentiation and maturation into functional tissue. During the differentiation stage, the lack of blood vessels often leads to hypoxia and associated necrosis within the deeper regions of the construct, especially where the diffusion distance is on the order of 100 μm or more (Lim

et al. 2015; Gholipourmalekabadi *et al*. 2016). The ability to understand and control physical–structural parameters of oxygen diffusion could have a major impact in the tissue engineering field and in clinical areas affected by chronic or acute hypoxia.

Timely subcellular delivery of adequate, but not too much, oxygen is also crucial to normal cellular physiology (Swartz, 1973), primarily due to its function in oxidative phosphorylation as an essential substrate for mitochondrial cytochrome *c* oxidase. Because of its key physiological and pathophysiological roles, the transport of oxygen has been studied extensively. Even so, the mechanism of transport from capillaries to tissue mitochondria is understood only superficially.

Computer simulation studies of membrane-level transport

Oxygen has generally been assumed to diffuse readily and passively through the capillary endothelium and through surrounding cell bodies, on its path to consumption in tissue mitochondria. The non-polarity and high lipid-solubility of oxygen suggests that it should generally pass through lipid bilayers without difficulty. High permeability of lipid bilayers to oxygen is consistent with Overton's rule, which states that the membrane permeability, P_M, of a molecule is directly proportional to its lipid–water partition coefficient, K_P, times its diffusion coefficient in the membrane, D_M, divided by the membrane thickness, h. The associated equation is $P_M = K_P D_M/h$ (Missner & Pohl, 2009). The partition coefficient is the ratio of the molecule's membrane solubility to its water solubility and serves as a measure of the tendency of the molecule to move spontaneously into the membrane from water. A related parameter is the free energy of transfer from water to lipid, ΔG_{tr}, which is essentially a log partition coefficient: $\Delta G_{tr} = -RT\ln K_P$, where R is the ideal gas constant and T is the absolute temperature. The partition coefficient and the diffusion coefficient (diffusivity) vary essentially independently.

While useful as a rule-of-thumb, Overton's rule usually provides only a rough estimate of the permeability, as lipid bilayers are inhomogeneous along the axis of permeation and show substantial variation in both the partition coefficient and the diffusion coefficient as a function of bilayer depth (Diamond & Katz, 1974). The free energy of transfer, ΔG_{tr}, likewise varies according to bilayer depth. In practice, the bilayer-depth region with the greatest concentration of the permeant is usually the region presenting least resistance to permeation (Diamond & Katz, 1974). Thus, accurate experimental estimation of K_P is often difficult to attain, due to limitations in sampling the permeant's concentration at all bilayer depths, especially where its solubility is lowest. For oxygen, the greatest resistances occur near the bilayer headgroups, where the phospholipid packing density is greatest (Diamond & Katz, 1974; Dotson *et al*. 2017).

Because the headgroup-associated barriers are generally rate-limiting for oxygen permeation through a lipid bilayer (Ghysels *et al*. 2017), experimental permeability estimates generally carry considerable uncertainty. In particular, estimates based on O_2 measurements using fluorescence probes or electron spin resonance (ESR) probes lack resolution in the highest-resistance headgroup regions (Widomska *et al*. 2007*b*; Kyrychenko & Ladokhin, 2013; do Canto *et al*. 2015; Angles *et al*. 2017; Dotson *et al*. 2017). However, bulk partition coefficients have been obtained for some membranes, yielding K_P values of 4−5 at 25−37°C (Möller *et al*. 2005, 2016; Möller & Denicola, 2018). These values are essentially the same as earlier olive oil–water partition coefficient measurements (Battino *et al*. 1983) and indicate that the average solubility of oxygen within lipid bilayers is greater than that in buffered water (Möller *et al*. 2005).

Atomistic computer modelling techniques, especially molecular dynamics simulations, provide a complement to experimental approaches. These techniques use biophysical models to enable study of membrane permeability and oxygen diffusional behaviour. The models are validated through comparison with experimental biophysical data for the membranes, as well as ESR and nuclear magnetic resonance oximetry data. Due to their atomic resolution, the simulations enable detailed mechanistic insight from a structural dynamics point of view. A key advantage is the ability to isolate molecular compositional variables and determine their influence on oxygen transport. Recent studies have addressed membrane cholesterol and transmembrane protein effects on the oxygen diffusional pathway and permeation kinetics, as well as anisotropic lateral diffusion along the midplane between the lipid leaflets.

Membrane cholesterol reduces permeability and enhances channelling. Cholesterol is a membrane compositional parameter important in cancers (Ding *et al*. 2019*b*). Dysregulation of cholesterol homeostasis is a common phenotype in solid tumours and can lead to increased membrane cholesterol levels (Li *et al*. 2006; Brown, 2007; Ding *et al*. 2019*b*). Most normal tissues have cholesterol content in the range 30−45% of the total lipid molecules (Weiner & Feigenson, 2018), while 50% cholesterol is normal for the lipid portion of red blood cell membranes and eye lens fibre cells (Jandl, 1996 and others reviewed in Widomska *et al*. 2007*b*).

A substantial body of work has examined the influence of membrane cholesterol on oxygen permeability and diffusion pathway (Subczynski *et al*. 1991; Dumas *et al*.

1997, 1999; Widomska *et al.* 2007*a*; Raguz *et al.* 2011; Angles *et al.* 2017; Plesnar *et al.* 2018; Angles and Pias, 2020; Dotson *et al.* 2020; Wang *et al.* 2020). Recent simulation studies have contributed several key findings. First, the overall oxygen lipid–water partition coefficient is reduced by 20−35% in membranes incorporating high levels of cholesterol (above 38%; Dotson *et al.* 2017, 2020). Yet, the local oxygen solubility is enhanced by cholesterol near the bilayer midplane, between the lipid leaflets (Dotson *et al.* 2017). Regardless of lipid composition, the bilayer midplane is typically characterized by a free energy well at the midplane, which is deepened with incorporation of saturated phospholipids and high levels of cholesterol (Subczynski *et al.* 1991; Dotson *et al.* 2017; De Vos *et al.* 2018*a*; Ghysels *et al.* 2019). Namely, high cholesterol content appears to promote physical 'channelling' of oxygen molecules toward the midplane (Fig. 1*B*) and to favour lateral diffusion within the bilayer, in the low-density region between the lipid layers (Dotson *et al.* 2017; Pias, 2020).

The permeability coefficient of the high-cholesterol bilayers is also reduced relative to pure phospholipid, but the magnitude of reduction is not consistently predicted from the average membrane–water partition coefficient, as would be expected according to a simple application of Overton's rule (Dotson *et al.* 2017, 2020). The divergence of partition coefficient and permeability coefficient indicates that diffusion-related effects may modify the permeability where higher cholesterol levels are present. This finding is somewhat unexpected, as previous studies have indicated that the transbilayer diffusion coefficient is not likely to be altered by cholesterol content but is governed primarily by the depth-dependent local partition coefficient (Zocher *et al.* 2013; Dotson *et al.* 2017). For carbon dioxide in high-cholesterol bilayers, Overton's rule has been shown to hold locally, where the membrane is segmented into several regions with distinct partition coefficients (Zocher *et al.* 2013). For oxygen in high-cholesterol bilayers, the rate of bilayer crossing may additionally be modulated by lateral diffusion near the midplane, increasing the transit time of oxygen molecules as they cross one leaflet, diffuse laterally, then exit across the second leaflet (De Vos *et al.* 2018*b*). Though accurate estimation of the lateral, or 'radial', oxygen diffusion coefficient is lacking as a direct function of bilayer cholesterol content, it appears that cholesterol enhances lateral diffusion (Dotson *et al.* 2017; Plesnar *et al.* 2018; Ghysels *et al.* 2019).

Such 'lateral transport' was proposed by Skulachev and indirectly supported by experimental ESR studies (Skulachev, 1990; Subczynski *et al.* 1991; Widomska *et al.* 2007*b*). Simulation studies indicate that lateral transport occurs due to a localized preference for radial movement, relative to transbilayer movement, in the interleaflet region (Ghysels *et al.* 2017, 2019). Diffusion coefficients for both transbilayer (normal) and lateral (parallel) movement are enhanced at the midplane, but the enhancement is greater for lateral diffusion. A clear explanation for this anisotropic diffusion coefficient enhancement is currently lacking. However, it

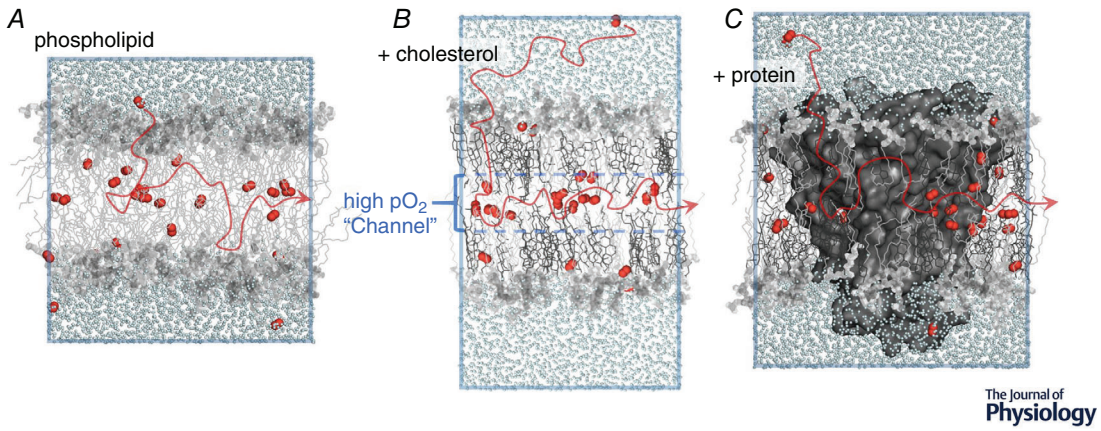

Figure 1. Molecular dynamics simulation models provide physical insight into O_2 permeation pathways and channelling toward the nonpolar membrane interior
Red lines and arrows illustrate possible O_2 molecule diffusion pathways across the bilayer headgroups and along the bilayer midplane, forming a high-P_{O_2} 'channel'. *A*, phospholipid bilayer composed of 1-palmitoyl-2-oleoylphosphatidylcholine (POPC). *B*, bilayer with 50% POPC and 50% cholesterol (1:1 molar ratio). *C*, potassium channel protein (PDB identifier 1R3J, Zhou & MacKinnon, 2003) imbedded in 50% POPC–50% cholesterol bilayer. All bilayers are hydrated, with explicit water molecules represented as reduced-size cyan spheres. O_2 shown as red spheres; POPC molecules in light grey; cholesterol molecules in dark grey; protein as dark grey surface; all H atoms hidden for clarity. Images are simulation snapshots associated with Dotson *et al*. (2020) and Dotson and Pias, 2018. PyMOL software (Schrödinger) used for imaging.

is clear that the enhancement is essentially independent of O_2 molecule confinement to the two-dimensional midplane, which relates to the free energy landscape and local partition coefficient rather than to the local diffusion coefficient. In phospholipid bilayer models lacking cholesterol, some O_2 molecules have been found to travel along the midplane at distances up to 10 times the bilayer thickness, in the absence of a concentration gradient (at equilibrium; De Vos *et al.* 2018*b*). Further investigation will likely reveal longer lateral transit distances within high-cholesterol membranes, especially under non-equilibrium steady-state conditions with a directional driving force.

Membrane proteins non-specifically reduce oxygen permeability. Together with cholesterol, transmembrane proteins constitute a critical structural–compositional factor. Although diverse proteins are ubiquitous in biological membranes, they have rarely been considered as a factor that could influence membrane permeability. Two experimental and one molecular dynamics simulation study have taken first steps toward determining the non-specific influence of transmembrane proteins on the oxygen permeability of membranes (Ashikawa *et al.* 1994; Subczynski *et al.* 2003; Dotson & Pias, 2018). The simulation study incorporated an ungated mouse potassium channel protein within model lipid bilayers of differing cholesterol content (Fig. 1*C*; Dotson & Pias, 2018). Membrane oxygen permeability was predicted to be reduced by a factor proportional to the area of the membrane occupied by protein (Dotson & Pias, 2018). This prediction is consistent with an experimental study using probe-based ESR with the transmembrane protein bacteriorhodopsin (Ashikawa *et al.* 1994). Both studies found the permeability of the lipid to be much greater than that of the protein, so that protein incorporation reduced the effective permeable area. This reduction is expected to be non-specific (Dotson & Pias, 2018) and may not be outweighed even by hypothesized protein-facilitated gas transport (due to access resistance; Hannesschlaeger *et al.* 2019).

In membranes incorporating protein, one might assume the permeability of the lipids themselves to be unchanged. However, the ESR and simulation studies both found the apparent permeability of the lipids to be reduced by the presence of protein, probably due to protein–lipid interfacial effects that have not been fully explained (Ashikawa *et al.* 1994; Dotson & Pias, 2018). These interfacial effects may involve the molecular dynamics of the lipids (Ashikawa *et al.* 1994), physical interaction of O_2 molecules with the surface of the protein (Dotson & Pias, 2018), and possibly also surface characteristics of the protein, such as surface roughness or sidechain length. Moreover, bacteriorhodopsin self-association and apparent phase separation into raft-like domains was found to modulate the protein's local effect on oxygen transport and permeability (Ashikawa *et al.* 1994). Additional investigation will be needed to understand the influence of protein abundance and organization on oxygen permeation as well as midplane lateral diffusion.

P_{O_2} gradients in cells and unstirred water layer effects

Several experimental studies used ESR spin probes to distinguish extracellular and intracellular oxygen concentrations (Hu *et al.* 1992; Liu *et al.* 1993; Khan *et al.* 2003; Shen *et al.* 2003). Large gradients were observed across the plasma membrane, with magnitudes dependent on the supplied oxygen partial pressure. In wild-type Chinese hamster ovary (CHO) cells, the extracellular-to-intracellular oxygen concentration gradient averaged ∼18% of the perfused molar O_2 concentration (Khan *et al.* 2003; Shen *et al.* 2003). The gradient increased to ∼30% in a mutant CHO cell line with significantly elevated plasma membrane cholesterol. Conversely, the gradient dropped to ∼10% in a mutant line with significantly reduced plasma membrane cholesterol (Khan *et al.* 2003). The nature of the gradients is puzzling and invites further investigation (Grinberg *et al.* 1998).

In particular, the oxygen solubility in cytosol, and the effective diffusion coefficient, may be lower than generally understood. Both cytosolic and interstitial fluids are aqueous and have usually been modelled as pure water or saline. However, they are colloidal suspensions rich in solutes – including salts, metabolites, proteins and other macromolecules. The fluids are interspersed inside solid matrices (Moeendarbary *et al.* 2013) consisting of macromolecular crowders and cytoskeletal or extracellular matrix structures. The solubility of oxygen in these solute-rich fluids would likely diminish relative to water or saline. Oxygen solubility is known to decline with increasing salinity (Battino *et al.* 1983), and solvation of proteins and metabolites may cause additional 'salting out' of oxygen (Zander, 1976, cited in Longmuir, 1981; Skulachev, 1990). Indeed, low oxygen solubility in cytosol may confer a biological advantage, as a means of guarding oxygen-sensitive enzymes and other macromolecules from poisoning or oxidative damage (Longmuir, 1981). To interpret the CHO cell oxygen gradients, it will be critical to determine the solubility of oxygen in the cytosol of intact cells, for which direct measurements are unfortunately lacking in the literature.

A 1989 review article on muscle oxygenation by Wittenberg and Wittenberg indicates very low oxygen solubility in the muscle cell sarcoplasm, a fluid substance resembling cytoplasm (Wittenberg & Wittenberg, 1989). The authors emphasize that sarcoplasmic P_{O_2}

remains nearly constant, at ∼3 Torr, over widely ranging muscle O_2 demand. Moreover, oxygen bound to myoglobin exceeds that free in the sarcoplasm by a ratio of 30:1, giving an approximate sarcoplasmic free O_2 concentration of ∼3.2 μM at 37°C. A major conclusion of the review is that two simultaneous and additive flows supply oxygen to mitochondria: dissolved oxygen flow and myoglobin-mediated oxygen delivery (via O_2-loaded myoglobin diffusion). Further, simple O_2 diffusion through the sarcoplasm cannot compensate for myoglobin-mediated delivery (Wittenberg & Wittenberg, 1989). Outside of muscle, myoglobin expression is extremely low, such that it does not aid in O_2 transport. However, the data on sarcoplasmic O_2 levels may well be relevant to non-muscle cytoplasms, where the solubility of O_2 likewise appears quite low.

The effective diffusion coefficient of oxygen in the tissue milieu may be impacted by macromolecular crowding as well as the large number of dissolved metabolites. Although macromolecular crowding is a more recently acknowledged phenomenon, structural and macromolecular components of tissue were already understood in the 1970s to influence the solubility and the diffusion coefficient of dissolved gases (Zander, 1975, cited in Vaupel, 1976). Indeed, Vaupel noted in 1976 that the water content of the diffusion medium alone was sufficient to predict the diffusion coefficient for oxygen. Specifically, he observed the O_2 diffusion coefficient to decrease exponentially with decreasing water content, independent of viscosity effects. In comparison with its reference value in 100 wt% water, the O_2 diffusion coefficient at 37°C was reduced by half in diffusion media containing 80 wt% water and further reduced to one-quarter the reference value at 65−70 wt% water (Vaupel, 1976).

Vaupel's observations point to a possible dependency of the effective O_2 diffusion coefficient on the extent of macromolecular crowding. Such a dependency is supported by a very recent study that used single-cell O_2 saturation fluorescence microscopy, combined with ultrarapid solution switching, to measure the kinetics of gas exchange in intact red blood cells (Richardson *et al.* 2020). The study concludes that oxygen diffusion is rate-limited by the cytoplasm, in a manner dependent on the diffusive path length (related to cell shape) and tortuosity (related to haemoglobin crowding). Although membrane barriers are not ruled out, the study suggests that the dominant barrier to gas exchange is the cytoplasm, with an O_2 diffusion coefficient approaching 70 $\mu m^2/s$ or less – nearly 30 times lower than the diffusion coefficient of oxygen in pure water (Richardson *et al.* 2020).

The presence of unstirred water layers surrounding the membrane must also be considered. Unstirred layers, or 'boundary layers', are regions unaffected by bulk convective motion, such as cytoplasmic streaming. Due to the local lack of convection, solute translocation in these layers is dominated by simple diffusion. For oxygen, the thickness of unstirred layers is expected to be on the order of 10 to more than 100 μm (Barry & Diamond, 1984; Levitt *et al.* 1988; Pohl *et al.* 1998; Dotson *et al.* 2017). Therefore, all water within the cell might be unstirred with respect to oxygen diffusion. It is unclear whether cytoplasmic streaming would be sufficiently convective to reduce the thickness of these layers (Hannesschlaeger *et al.* 2019). Even so, they would likely be very thick (e.g. 10−30 μm), compared with the few-nanometre thickness of individual membranes (∼6 nm or 0.006 μm). The influence of cholesterol on the oxygen concentration would, thus, be localized to the immediate vicinity of the membrane and should fall off quickly in the adjacent unstirred water layers (Dotson *et al.* 2017). The lipid bilayer permeability studies discussed above indicate that the cholesterol content of the plasma membrane alone would not be sufficient to generate the large oxygen gradients observed in the CHO cells, as the permeability of even very high-cholesterol membranes has been found to be of the same order of magnitude as unstirred water (Dotson *et al.* 2017, 2020; Widomska *et al.* 2007*b*).

Understanding the ESR spin probe location will also be important for interpreting the gradients. The extracellular probe lithium phthalocyanine is crystalline and appears to measure in the aqueous phase. In contrast, the intracellular probe ^{15}N-PDT is a tempone and may preferentially localize to the membrane vicinity (Polnaszek *et al.* 1978), even though it lacks a lipid anchor and appears not to have been intentionally targeted to the membrane. Specifically, the tempone likely reports on the oxygen concentration in the membrane polar region just beneath the headgroups and, therefore, would avoid the flanking unstirred layer on the intracellular side (Polnaszek *et al.* 1978; Kyrychenko and Ladokhin, 2013; Angles *et al.* 2017). If so, the gradients may, indeed, reflect the permeability of the plasma membrane. While it is probable that the permeability of the extracellular unstirred water layer would also contribute to the gradients, substantial modulation of the gradient magnitude by the cholesterol content (Khan *et al.* 2003) suggests that the unstirred layer did not dominate the measurements.

Regardless of the nature of the CHO cell oxygen gradients, understanding the resistance to oxygen permeation presented by aqueous fluids in and around cells will be essential to accurately assessing oxygen availability. Indeed, recent work in cell culture indicates that slow oxygen diffusion through aqueous media leads to wide variability in molar O_2 concentration at the cellular level, ranging from hyperoxia to near-anoxia (Place *et al.* 2017). Similar variability occurs in engineered tissue constructs and can critically regulate cell death and differentiation (Csete, 2005; Gholipourmalekabadi *et al.* 2016).

Oxygen channelling along lipid-based pathways

Most often, oxygen has been assumed to diffuse across cell bodies, likely because this pathway would appear to traverse the shortest distance. Figure 2 represents transport along cell bodies as pathway 1, while an alternative route through interstitial fluid is depicted as pathway 2. A third, and possibly preferential, route through networked lipids is illustrated as pathway 3.

In diffusing across cell bodies, oxygen would encounter many membrane-associated barriers. While the plasma membrane alone would be unlikely to limit the diffusion rate, the cellular milieu is exceedingly rich in organellar membranes, especially those of the endoplasmic reticulum and mitochondrial networks. Organellar compartments, cytoskeletal structures and macromolecules would present additional barriers. Therefore, oxygen diffusing across cell bodies would encounter resistance from the low-solubility aqueous cytoplasm, from multiple membranes, and from other cellular structures as well as macromolecular crowders. While the interstitium (pathway 2) lacks some of the obstacles, it, too, is rich with fibrous extracellular matrix structures and soluble proteins. The cells of healthy tissues are interconnected through junctions, leaving narrow and confined spaces for potential oxygen diffusion. Along either pathway 1 or 2, steering around the obstacles would substantially lengthen the diffusion path.

Pathway 3, through networked lipids, is supported by the preferential solubility of oxygen in lipids *versus* water, anisotropically enhanced lateral diffusion of oxygen near the midplane of lipid bilayers, and continuous networks of membranes and lipid droplets within and among cells of healthy tissues. Compared with water or aqueous buffer, oxygen solubility is greater by a factor of 3–5 for whole membranes (Möller *et al.* 2005, 2016; Möller & Denicola, 2018) and by a factor of 10 or more near the bilayer midplane (Al-Abdul-Wahid *et al.* 2006). Oxygen has been reported by Longmuir, citing Krogh (1929), to be 'virtually insoluble in cytosol', and Longmuir's own measurements in cells indicate a factor of 25 enhancement of oxygen solubility in localized, lipid-based 'channels of high solubility' (Benson *et al.* 1980; Longmuir, 1981; Longmuir *et al.* 1981).

Along pathway 3, the resistance of low-solubility aqueous fluids would be reduced by shortening the distance travelled within them. Inside membranes, the local diffusion coefficient is enhanced anisotropically, to favour lateral diffusion (Fig. 1; Ghysels *et al.* 2017; De Vos *et al.* 2018*b*). The presence of transmembrane proteins, especially within ordered microdomains (rafts), could present physical obstacles to slow diffusive progress. However, even ordered raft *lipids* may facilitate channelling along the midplane (Ghysels *et al.* 2019). In such a lipid-dominated diffusion scheme, the lipids would serve primarily to accelerate oxygen diffusion, by reducing the path-length of diffusion through resistant aqueous fluids and by providing 'channels' of high solubility and enhanced diffusion coefficient. Experimental evidence of accelerated oxygen diffusion via networked lipids has been reported in lung surfactant (Olmeda *et al.* 2010).

Given thin separations of several to tens of nanometres at junction points between cells and organelles (Helle *et al.* 2013; Maeda *et al.* 2009), the associated unstirred water

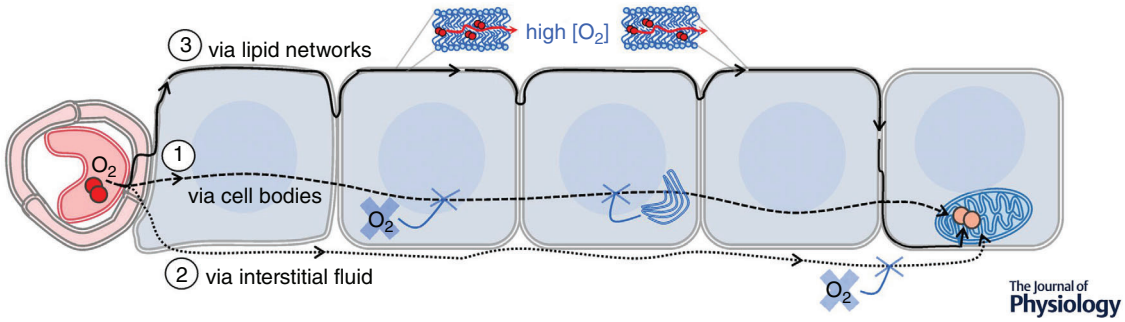

Figure 2. Pathway of oxygen diffusion from a red blood cell, across the capillary endothelium, into surrounding cells
Some oxygen must reach mitochondria several cell layers away. The preferential pathway is unknown, and three potential pathways are illustrated. Pathway 1: diffusion across cell bodies. Oxygen has often been assumed to diffuse across cell bodies, primarily via the cytosol. Opposing factors include low oxygen solubility in cytosol and intervening subcellular structures such as membranous organelles. Pathway 2: diffusion via interstitial fluid. A potential advantage of interstitial fluid over cytosol is the absence of organelles and associated membrane barriers. However, this pathway is disfavoured by low oxygen solubility in aqueous fluids and by limited extracellular space between cells. Pathway 3: diffusion via lipid networks. This route appears to be the preferential pathway for oxygen diffusion within tissue, due to greatly enhanced oxygen solubility in lipids and a locally enhanced diffusion coefficient near the midplane of lipid bilayers ('channelling', as in Fig. 1). The number of membrane-associated barriers encountered on this pathway would be lower than the number encountered in crossing cell bodies. Membrane proteins may tend to reduce the rate of diffusion within lipid bilayers.

layers along pathway 3 would be equally thin. As such, membrane headgroup-associated barriers may become rate-limiting, along with the intermembrane unstirred layers (depending on their thickness). Membrane compositional effects on the permeability of the lipid layers and on the ease of lateral diffusion at the midplane would likely influence the rate of oxygen supply in support of metabolism.

Figure 3 illustrates potential lipid-based diffusion pathways *within* cells, as proposed by various researchers. The figure highlights the low solubility of oxygen in cytosol and visualizes accelerated diffusion through the endoplasmic reticulum, mitochondrial networks and neutral lipid droplets. Sufficiently fluid neutral lipid droplets may facilitate oxygen diffusion (Desaulniers *et al.* 1996; Sidell, 1998), while highly ordered ones may present obstacles.

Quantitative comparison of pathway permeabilities

In this section, we develop a simple quantitative model to estimate the oxygen permeability associated with each of the three pathways illustrated in Fig. 2. For tissue components in series, the inverse of the total permeability, $1/P_{tot}$, can be calculated as the sum of the inverse permeabilities of all the components (Diamond & Katz, 1974). The inverse permeability is a resistance, sometimes called 'resistance to permeation' (Widomska *et al.* 2007b), and is here designated $R_{tot} = 1/P_{tot}$. For a simple quantitative model of the pathways in Fig. 2, the tissue components can be treated as two kinds: unstirred aqueous fluid components and membrane components. In pathways 1 and 2, membranes are treated solely as 'barriers' to oxygen diffusion, while in pathway 3, they also act as conduits for oxygen diffusion along the bilayer midplane. Note that cytoskeletal and extracellular matrix components, as well as various macromolecular and solute components, are neglected in this model because their influence on permeability is poorly understood.

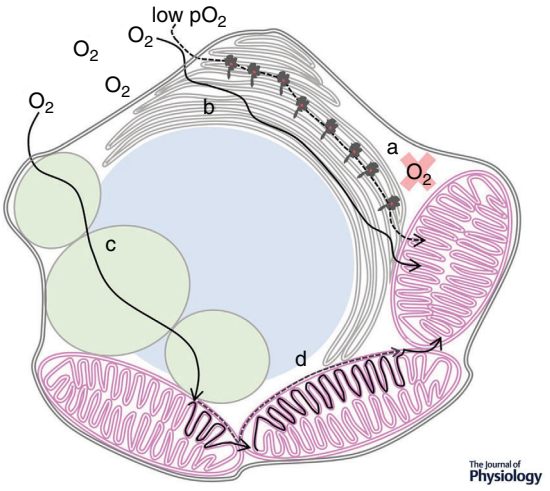

Figure 3. High-solubility, lipid-based pathways within cells
(a) Very low oxygen solubility in cytosol, reported by Longmuir (1981) and Krogh (1929, cited in Longmuir, 1981). The solubility of oxygen in cytosol is expected to be lower than in saline and at least 5 times lower than in lipid. (b) High-solubility 'channels' likely formed by the endoplasmic reticulum and possibly facilitated at low P_{O_2} by haem-bearing cytochrome P450 molecules (dashed line), proposed by Longmuir (1981). (c) Accelerated oxygen diffusion via lipid droplets (green), proposed by Skulachev (1990) and supported by Sidell (Desaulniers *et al.* 1996; Sidell, 1998). (d) Lateral diffusion within mitochondrial membranes, proposed by Skulachev (1990) and supported by Sidell (1998) and Popel (Dutta & Popel, 1995).

Table 1. Coefficients and pathway lengths assumed in the quantitative model for each pathway (pwy)

Pathway	m	n	s	L_{pwy} (μm)
1	1.7×10^4	88	0	86
2	1.8×10^4	6	0	95
3	9	10	2.2×10^4	110

Permeability coefficient values are available for individual membranes and for water layers and midplane segments of the same thickness as a membrane. To use the available values, the total pathway resistance and permeability are estimated from the sum of a series of fixed-thickness aqueous and membrane components:

$$R_{tot} = \frac{1}{P_{tot}} = \frac{m}{P_{aq}} + \left(\frac{n}{P_M} + \frac{s}{P_{||}}\right) \quad (1)$$

m, n and s are coefficients representing the number of fixed-thickness segments of each type in a pathway. The permeability coefficients for the component fixed-thickness segments are P_{aq}, P_M, and $P_{||}$. P_M is the transverse permeability for oxygen molecules crossing a lipid bilayer membrane, sometimes called $P_\perp$ (Ghysels *et al.* 2017). $P_{||}$ represents the oxygen permeability of the midplane region parallel to the lipid leaflets (Ghysels *et al.* 2017), having a thickness equal to the headgroup-to-headgroup membrane thickness (~5 nm). P_{aq} is the permeability of an aqueous layer of the same thickness (~5 nm). The coefficient m is the number of ~5 nm aqueous segments; n is the number of membrane barriers; and s the number of membrane midplane segments – only relevant to the hydrophobic channel portion of pathway 3.

Table 1 provides the values of m, n and s for each pathway in Fig. 2, along with the associated total pathway length, L_{pwy}. Where the coefficient values are relatively small (<100), they were determined by estimating the number of membrane barriers or thin aqueous layers traversed along the given pathway, as illustrated in Fig. 2. Where large (>100), they were calculated from estimates of the overall distance travelled, divided by

Table 2. Effect of aqueous fluid permeability (P_{aq}) on estimated resistance and permeability for oxygen diffusing along the various pathways illustrated in Fig. 2, with all membranes modelled as simple POPC bilayers

Model fluid	P_{aq} (cm/s)	Pathway	R_{tot} (s/cm)	P_{tot} (cm/s)	tau (s)	
Pure water						
(i) Sim. water[a]	116	1	150	6.9×10^{-3}	1.3	
		2	160	6.4×10^{-3}	1.5	
		3	600	1.7×10^{-3}	6.7	Rate-influencing
(ii) Expt. water[b]	41	1	410	2.4×10^{-3}	3.5	
		2	450	2.2×10^{-3}	4.3	
		3	600	1.7×10^{-3}	6.7	Rate-influencing
Longmuir cytosol[c]						
(iii) (Sim. water)÷3	116÷3	1	430	2.3×10^{-3}	3.7	
		2	470	2.1×10^{-3}	4.5	
		3	600	1.7×10^{-3}	6.7	Rate-influencing
(iv) (Expt. water)÷6	41÷6	1	2400	4.1×10^{-4}	21	
		2	2700	3.7×10^{-4}	26	
		3	600	1.7×10^{-3}	6.7	Preferential
(v) (Sim. POPC)÷25	26÷25	1	16,000	6.3×10^{-5}	140	
		2	18,000	5.7×10^{-5}	170	
		3	610	1.6×10^{-3}	6.8	Preferential

POPC permeability values from De Vos *et al*. 2018*b*: 26 cm/s for transbilayer O_2 diffusion, P_M, and 36 cm/s for radial diffusion along bilayer midplane, $P_{||}$, with segment thickness equal to bilayer thickness, 5.2 nm. Specified model fluid is used to represent both intracellular and extracellular aqueous fluids for each calculation, with aqueous fluid permeability P_{aq}. Resistance is total resistance to permeation for the pathway (pwy), R_{tot}, calculated using eqn (1). P_{tot} is total pathway permeability, $P_{tot} = 1/R_{tot}$. The time parameter tau is the product $R_{tot}L_{pwy}$. Calculations assume 37°C.

[a] Simulation-based permeability coefficient for water layer 5.2 nm thick (Ghysels *et al*. 2017), similar in thickness to a lipid bilayer.

[b] Water permeability coefficient from Ghysels *et al*. 2017, using experimental data in Ju and Ho, 1989. Value adjusted to 5.2 nm thickness.

[c] Approximations of 25 times lower solubility of O_2 in cytosol, relative to lipid, as discussed in Longmuir, 1981, referencing Benson *et al*. 1980, and Longmuir *et al*. 1981. (Sim. water)/3 assumes a simulation POPC-water partition coefficient $K_P = 8$, as estimated for a similar model (Dotson *et al*. 2017). (Expt. water)/6 assumes POPC-water $K_P = 4$, as for EYPC liposomes (Möller *et al*. 2005). (Sim. POPC)/25 estimates aqueous fluid permeability as 1/25 the permeability of a POPC bilayer (based on simulations by De Vos *et al*. 2018*b*).

the fixed ∼5 nm increment. As a rough estimate, oxygen molecules traveling across cell bodies (pathway 1) were assumed to encounter 20 membrane barriers per cell, including 18 organellar membranes (primarily endoplasmic reticulum). This value is intended as a lower-end approximation, based on the author's observation of transmission electron micrographs of a variety of cell types. The cells beyond the endothelial layer were treated as spherical in shape, with 20 μm diameters. Using the model in eqn (1), the total resistance, total permeability and a time parameter, tau, were calculated based on various theoretical and experimental estimates for membrane and aqueous fluid permeability. Calculations using this model give the data presented in Tables 2 and 3.

Table 2 highlights the significance of the aqueous fluid permeability in determining the total permeability, especially for pathways 1 and 2. As discussed earlier, the solubility of oxygen in cytosol and interstitial fluid is poorly understood. Yet, the calculations demonstrate that the solubility of oxygen in cytosol relative to lipids is paramount to determining the preferential diffusion pathway.

As an upper-limit estimate of aqueous fluid oxygen solubility, the 'model fluid' was first taken to have an oxygen permeability, P_{aq}, equal to that of pure water ((i) and (ii) in Table 2). Recall that the relative solubility, or partition coefficient, is directly proportional to the permeability coefficient, according to Overton's rule. Using a pure water permeability estimate from a recent simulation study ((i) Sim. water; Ghysels *et al*. 2017), the resulting total resistance, R_{tot}, and total permeability, P_{tot}, for pathways 1 and 2 are similar, as is the time parameter tau, which is the product of the total resistance and the total pathway length. It should be noted that tau may have no direct physical meaning, though it is used here as a proxy for oxygen transit time. For both of these aqueous-fluid-dominated pathways, tau is more than 4 times smaller than it is for lipid-dominated pathway 3. This finding is consistent with the widely accepted assumption that oxygen diffusion through cell bodies or interstitial fluid is the dominant pathway. A similar result is obtained using an experimental oxygen permeability estimate for pure water (Ghysels *et al*. 2017, based on data from Ju & Ho, 1989), except that the preference

Table 3. Effect of membrane permeability coefficients P_M and $P_{||}$ on estimated resistance and permeability for oxygen diffusing along pathway 3 (Fig. 2), using aqueous model fluid (v) (Table 2)

Membrane model	P_M (cm/s)	$P_{||}$ (cm/s)	R_{tot} (s/cm)	P_{tot} (cm/s)	tau (s)
Simulation					
POPC[a]	26	36	610	1.6×10^{-3}	6.8
DOPC[a]	39	41	540	1.9×10^{-3}	6.0
POPC/cholesterol[b]	22	44	500	2.0×10^{-3}	5.6
POPC/protein[c]	13	18	1200	8.5×10^{-4}	13
Experiment					
POPC[d]	157.4	157.4	137	7.3×10^{-3}	1.5
POPC/cholesterol[d]	49.7	49.7	435	2.3×10^{-3}	4.8

Permeability values based on molecular dynamics simulation data (upper part of table) or on ESR experimental data (lower part).
[a] Dioleoylphosphatidylcholine (DOPC) phospholipid. P_M and $P_{||}$ from De Vos *et al*. 2018*a*.
[b] 50% cholesterol and 50% POPC (1:1 molar ratio). P_M from Dotson *et al*. 2017. $P_{||}$ estimated by relating the $P_{||}$ enhancement for POPC in De Vos *et al*. 2018*a*, to the oxygen transport parameter curve in Dotson *et al*. 2017, then extending the comparison to the POPC/cholesterol P_M value and oxygen transport parameter curve in Dotson *et al*. 2017.
[c] P_M from Dotson and Pias, 2018, for ∼30 wt% transmembrane protein (mouse K^+ channel). $P_{||}$ enhancement estimated as ∼38%, based on the enhancement for POPC in De Vos *et al*. 2018*a*.
[d] P_M from Widomska *et al*. 2007*b*. The associated ESR technique does not discern whether $P_{||}$ would be enhanced relative to P_M. Hence, the two values have been treated as equal.

for aqueous-dominated diffusion is less pronounced ((ii) Expt. water).

Three additional 'model fluids' were devised, in an attempt to better approximate the solubility of oxygen in biological fluids ((iii), (iv) and (v) in Table 2). All are based on Longmuir's finding that oxygen is ∼25 times more soluble in lipids than in cytosol. First, model fluid (iii) reduces the simulation-based pure water oxygen permeability by a factor of 3, accounting for an exaggerated simulation estimate of the membrane–water partition coefficient, $K_P = 8$, giving a total factor of 24 difference between the model fluid and lipid permeabilities. This adjustment makes P_{aq} approximately the same as with model fluid (ii), and the results are similar to those estimated with the pure-water models. Second, model fluid (iv) uses an experimentally estimated membrane–water partition coefficient, $K_P = 4$, and reduces the experiment-based pure water oxygen permeability by a factor of 6 to give a total factor of 24 difference between the model fluid and lipid permeabilities. This adjustment leads to a factor of 6 increase in the resistance and the time parameter tau, suggesting that the lipid-based pathway 3 may be faster than the water-dominated pathways by a factor of ∼3.5. Finally, model fluid (v) provides a lower-limit estimate of oxygen solubility in biological aqueous fluid, approximating the model fluid permeability as 1/25 the simulation-based permeability of a lipid bilayer (De Vos *et al*. 2018*b*). This model leads to resistance and tau values ∼20 times greater for the water-dominated pathways than for lipid-based pathway 3.

While care must be taken to remain aware of the many assumptions made in the model, these findings suggest that the solubility of oxygen in cytoplasm and interstitial fluid is, indeed, a critical parameter that could modulate the diffusion pathway preference within tissue. Low cytosolic oxygen solubility of the order observed by Longmuir would suggest that high-solubility, lipid-based pathways may accelerate oxygen diffusional delivery and may even become rate-limiting. Even with modest estimates of oxygen solubility in biological fluids (models (i), (ii) and (iii)), the values of tau are similar enough for all pathways to suggest that oxygen diffusion along the lipid-based pathway may contribute ∼20−30% of the oxygen delivered and, thus, may influence the rate of oxygen delivery, even if it is not the preferential pathway.

It is interesting to note that the various model fluid oxygen permeabilities, and related solubilities, do not influence the value of tau for pathway 3, though the aqueous permeabilities themselves vary over a range of 2 orders of magnitude. This is because the unstirred aqueous layers along pathway 3 are thin and few in number and, hence, have minimal influence on the overall rate of oxygen transfer via the lipid-based pathway.

Given that lipid-based pathway 3 may be preferential where the aqueous fluid oxygen solubility is quite low (model fluids (iv) and (v) in Table 2), it is reasonable to consider whether variations in membrane permeability due to compositional factors could influence oxygen flux along pathway 3. Table 3 compares the calculated pathway total resistance, total permeability, and time parameter tau for pathway 3, using permeability estimates from molecular dynamics simulations and from ESR experiments. The potential effects of phospholipid type, cholesterol and membrane protein content are considered.

Holding the aqueous fluid permeability constant but varying the membrane permeability does influence the calculated parameters. Among the calculations using simulation-based permeability values (upper part of Table 3), the variations due to bilayer lipid composition are relatively small (±20−25%). Given the many assumptions in the model, it is difficult to discern whether these differences would be significant. Still, the magnitude of variation is consistent with experimentally observed changes due to cholesterol in cellular oxygen concentration gradients and red blood cell oxygen uptake and release rates (Khan *et al.* 2003; Menchaca *et al.* 1998). Introduction of ∼30 wt% protein within a POPC bilayer reduces pathway 3 total permeability by half, and nearly doubles the time parameter tau. However, it should be noted that the midplane permeability, $P_{||}$, for the protein-incorporating membrane model is unknown and has been estimated with the assumption that it will scale in the same way $P_{||}$ scales relative to P_M for pure POPC. It is possible that $P_{||}$ may be substantially higher (or lower) than assumed.

Using experimental ESR-based estimates of POPC and POPC/cholesterol permeability gives different values for the calculated parameters (lower part of Table 3). These calculations suggest that oxygen transit along the lipid-based pathway 3 would be accelerated relative to either aqueous-fluid-based pathway, 1 or 2, even with the upper-limit assumption that cytosol and interstitial fluid have permeability equal to that of pure water (experimental model fluid (ii) in Table 2). Note that the calculated parameters for pathways 1 and 2 are unaffected by substitution of the ESR-derived POPC permeability for the simulation-based value (data not shown). Incorporation of cholesterol in a 1:1 molar ratio with POPC (50 mol%) reduces the acceleration along pathway 3, rendering the lipid-based pathway similar in permeability to pathways 1 and 2.

The quantitative modelling presented here leads to the conclusion that diffusion along lipid-based pathways is likely to influence the rate of oxygen delivery within tissues for all model fluid and model membrane combinations examined. Knowing the oxygen solubility of interstitial and cytosolic fluids will be critical to determining whether lipid-based pathways are preferential (rate-limiting) or exert a minor influence on oxygen diffusional delivery (±10−45%). The effects of ever-present membrane proteins require additional study, especially with regard to possible influence on oxygen diffusion along the bilayer midplane ($P_{||}$) as well as the influence of membrane protein crowding and organization.

Conclusion and outlook

Oxygen availability depends on the path of its diffusion from blood capillaries to sites of consumption within tissue. Cumulative evidence suggests that the molecular structures of tissue, especially cellular membranes, can influence the rate of oxygen diffusive delivery. Lipids may act primarily as accelerants, to overcome aqueous barriers generated by low oxygen solubility and, thus, high resistance. Minimizing the thickness of aqueous layers may promote rapid 'channelling' of oxygen along high-solubility pathways. The solubility is especially high near the midplane of lipid bilayers, between the lipid leaflets, and cholesterol enhances the channelling effect. The oxygen diffusion coefficient is, likewise, enhanced near the midplane, in an anisotropic manner favouring lateral diffusion between the lipid layers. Both cholesterol and transmembrane proteins reduce oxygen transbilayer permeability and may modulate the rate of oxygen transit across cells and tissues if the preferential diffusion pathway is lipid-dominated.

Experiments to determine a preferential diffusion pathway will be difficult because oxygen propagates on an extremely rapid time scale, and distinguishing the pathway may require probe-based techniques fraught with uncertainty. Further, molecular probes usually confound solubility and diffusion effects. Accurate measurement of the oxygen solubility in the cytosol of intact cells would be a major contribution toward understanding the pathway and would also help interpret experimental data suggesting large concentration gradients may exist within cells. Probe-free measurements of movement within and across lipids can easily be confounded by unstirred layer artefacts, adding further challenge to the experiments.

However, intracellular oxygen availability has great physiological and pathophysiological significance, especially in tumours and engineered tissues. A goal of ongoing work should be to determine whether oxygen availability can be influenced by structural–compositional features of tissues, such as interstitial fluid fraction, cellular connectivity and lipid composition. If so, knowledge of the modulating factors could reveal therapeutic strategies as well as approaches to controlling cellular oxygenation in the laboratory.

References

Al-Abdul-Wahid MS, Yu C-H, Batruch I, Evanics F, Pomes R & Prosser RS (2006). A combined NMR and molecular dynamics study of the transmembrane solubility and diffusion rate profile of dioxygen in lipid bilayers. *Biochemistry* **45**, 10719–10728.

Angles G, Dotson R, Bueche K & Pias SC (2017). Predicted decrease in membrane oxygen permeability with addition of cholesterol. *Adv Exp Med Biol* **977**, 9–14.

Angles G & Pias SC (2020). Discerning membrane steady-state oxygen flux by Monte Carlo Markov chain modeling. *Adv Exp Med Biol* **1269**, (in press).

Ashikawa I, Yin JJ, Subczynski WK, Kouyama T, Hyde JS & Kusumi A (1994). Molecular organization and dynamics in bacteriorhodopsin-rich reconstituted membranes: Discrimination of lipid environments by the oxygen transport parameter using a pulse ESR spin-labeling technique. *Biochemistry* **33**, 4947–4952.

Barry PH & Diamond JM (1984). Effects of unstirred layers on membrane phenomena. *Physiol Rev* **64**, 763–872.

Battino R, Rettich TR & Tominaga T (1983). The solubility of oxygen and ozone in liquids. *J Phys Chem Ref Data* **12**, 163–178.

Benson DM, Knopp JA & Longmuir IS (1980). Intracellular oxygen measurements of mouse liver cells using quantitative fluorescence video microscopy. *Biochim Biophys Acta* **591**, 187–197.

Brown AJ (2007). Cholesterol, statins and cancer. *Clin Exp Pharmacol Physiol* **34**, 135–141.

Carreau A, El Hafny-Rahbi B, Matejuk A, Grillon C & Kieda C (2011). Why is the partial oxygen pressure of human tissues a crucial parameter? Small molecules and hypoxia. *J Cell Mol Med* **15**, 1239–1253.

Cavallaro U & Christofori G (2001). Cell adhesion in tumor invasion and metastasis: Loss of the glue is not enough. *Biochim Biophys Acta* **1552**, 39–45.

Cicco G, Giorgino F & Cicco S (2011). Wound healing in diabetes: Hemorheological and microcirculatory aspects. *Adv Exp Med Biol* **701**, 263–269.

Colliez F, Gallez B & Jordan BF (2017). Assessing tumor oxygenation for predicting outcome in radiation oncology: A review of studies correlating tumor hypoxic status and outcome in the preclinical and clinical settings. *Front Oncol* **7**, 10.

Csete M (2005). Oxygen in the cultivation of stem cells. *Ann N Y Acad Sci* **1049**, 1–8.

Desaulniers N, Moerland TS & Sidell BD (1996). High lipid content enhances the rate of oxygen diffusion through fish skeletal muscle. *Am J Physiol* **271**, R42–R47.

De Vos O, Hecke TV & Ghysels A (2018*a*). Effect of chain unsaturation and temperature on oxygen diffusion through lipid membranes from simulations. *Adv Exp Med Biol* **1072**, 399–404.

De Vos O, Venable RM, Van Hecke T, Hummer G, Pastor RW & Ghysels A (2018*b*). Membrane permeability: Characteristic times and lengths for oxygen and a simulation-based test of the inhomogeneous solubility-diffusion model. *J Chem Theory Comput* **14**, 3811–3824.

Diamond JM & Katz Y (1974). Interpretation of nonelectrolyte partition coefficients between dimyristoyl lecithin and water. *J Membr Biol* **17**, 121–154.

Ding L, Su Y, Fassl A, Hinohara K, Qiu X, Harper NW, Huh SJ, Bloushtain-Qimron N, Jovanović B, Ekram M, Zi X, Hines WC, Alečković M, Gil del Alcazar C, Caulfield RJ, Bonal DM, Nguyen Q-D, Merino VF, Choudhury S, Ethington G, Panos L, Grant M, Herlihy W, Au A, Rosson GD, Argani P, Richardson AL, Dillon D, Allred DC, Babski K, Kim EMH, McDonnell CH, Wagner J, Rowberry R, Bobolis K, Kleer CG, Hwang ES, Blum JL, Cristea S, Sicinski P, Fan R, Long HW, Sukumar S, Park SY, Garber JE, Bissell M, Yao J & Polyak K(2019*a*). Perturbed myoepithelial cell differentiation in BRCA mutation carriers and in ductal carcinoma in situ. *Nat Commun* **10**, 4182.

Ding X, Zhang W, Li S & Yang H (2019*b*). The role of cholesterol metabolism in cancer. *Am J Cancer Res* **9**, 219–227.

do Canto MA, Santos PD, Martins J & Loura LM (2015). Behaviour of pyrene as a polarity probe in palmitoylsphingomyelin and palmitoylsphingomyelin/cholesterol bilayers: A molecular dynamics simulation study. *Colloids Surf A* **480**, 296–306.

Dotson RJ, McClenahan E & Pias SC (2020). Updated evaluation of cholesterol's influence on membrane oxygen permeability. *Adv Exp Med Biol* **1269**, (in press).

Dotson RJ & Pias SC (2018). Reduced oxygen permeability upon protein incorporation within phospholipid bilayers. *Adv Exp Med Biol* **1072**, 405–411.

Dotson RJ, Smith CR, Bueche K, Angles G & Pias SC (2017). Influence of cholesterol on the oxygen permeability of membranes: Insight from atomistic simulations. *Biophys J* **112**, 2336–2347.

Dumas D, Latger V, Viriot ML, Blondel W & Stoltz JF (1999). Membrane fluidity and oxygen diffusion in cholesterol-enriched endothelial cells. *Clin Hemorheol Microcirc* **21**, 255–261.

Dumas D, Muller S, Gouin F, Baros F, Viriot ML & Stoltz JF (1997). Membrane fluidity and oxygen diffusion in cholesterol-enriched erythrocyte membrane. *Arch Biochem Biophys* **341**, 34–39.

Dutta A & Popel AS (1995). A theoretical analysis of intracellular oxygen diffusion. *J Theor Biol* **176**, 433–445.

Elas M, Williams BB, Parasca A, Mailer C, Pelizzari CA, Lewis MA, River JN, Karczmar GS, Barth ED & Halpern HJ (2003). Quantitative tumor oxymetric images from 4D electron paramagnetic resonance imaging (EPRI): Methodology and comparison with blood oxygen level-dependent (BOLD) MRI. *Magn Reson Med* **49**, 682–691.

Gholipourmalekabadi M, Zhao S, Harrison BS, Mozafari M & Seifalian AM (2016). Oxygen-generating biomaterials: A new, viable paradigm for tissue engineering? *Trends Biotechnol* **34**, 1010–1021.

Ghysels A, Krämer A, Venable RM, Teague WE, Lyman E, Gawrisch K & Pastor RW (2019). Permeability of membranes in the liquid ordered and liquid disordered phases. *Nat Commun* **10**, 5616.

Ghysels A, Venable RM, Pastor RW & Hummer G (2017). Position-dependent diffusion tensors in anisotropic media from simulation: Oxygen transport in and through membranes. *J Chem Theory Comput* **13**, 2962–2976.

Grinberg OY, James PE & Swartz HM (1998). Are there significant gradients of pO_2 in cells? *Adv Exp Med Biol* **454**, 415–423.

Hall E (2006). *Radiobiology for the Radiologist*, 6th edn. Lippincott Williams & Wilkins, Philadelphia.

Hannesschlaeger C, Horner A & Pohl P (2019). Intrinsic membrane permeability to small molecules. *Chem Rev* **119**, 5922–5953.

Helle SCJ, Kanfer G, Kolar K, Lang A, Michel AH & Kornmann B (2013). Organization and function of membrane contact sites. *Biochim Biophys Acta* **1833**, 2526–2541.

Höckel M, Schlenger K, Mitze M, Schäffer U & Vaupel P (1996). Hypoxia and radiation response in human tumors. *Semin Radiat Oncol* **6**, 3–9.

Hou H, Lariviere JP, Demidenko E, Gladstone D, Swartz H & Khan N (2009). Repeated tumor pO_2 measurements by multi-site EPR oximetry as a prognostic marker for enhanced therapeutic efficacy of fractionated radiotherapy. *Radiother Onco* **91**, 126–131.

Hu H, Sosnovsky G & Swartz HM (1992). Simultaneous measurements of the intra- and extra-cellular oxygen concentration in viable cells. *Biochim Biophys Acta* **1112**, 161–166.

Jakab K, Norotte C, Marga F, Murphy K, Vunjak-Novakovic G & Forgacs G (2010). Tissue engineering by self-assembly and bio-printing of living cells. *Biofabrication* **2**, 022001.

Jandl JH (1996). *Blood: Textbook of Hematology*, pp. 853–901. Little, Brown and Company, Boston.

Ju L-K & Ho CS (1989). Oxygen diffusion coefficient and solubility in *n*-hexadecane. *Biotechnol Bioeng* **34**, 1221–1224.

Kalogeris T, Baines CP, Krenz M & Korthuis RJ (2016). Ischemia/reperfusion. *Compr Physiol* **7**, 113–170.

Khan N, Shen J, Chang TY, Chang CC, Fung PC, Grinberg O, Demidenko E & Swartz H (2003). Plasma membrane cholesterol: A possible barrier to intracellular oxygen in normal and mutant CHO cells defective in cholesterol metabolism. *Biochemistry* **42**, 23–29.

Krogh A (1929). *The Anatomy and Physiology of Capillaries*. Yale University Press, New Haven.

Kyrychenko A & Ladokhin AS (2013). Molecular dynamics simulations of depth distribution of spin-labeled phospholipids within lipid bilayer. *J Phys Chem B* **117**, 5875–5885.

Levitt MD, Kneip JM & Levitt DG (1988). Use of laminar flow and unstirred layer models to predict intestinal absorption in the rat. *J Clin Invest* **81**, 1365–1369.

Li YC, Park MJ, Ye S-K, Kim C-W & Kim Y-N (2006). Elevated levels of cholesterol-rich lipid rafts in cancer cells are correlated with apoptosis sensitivity induced by cholesterol-depleting agents. *Am J Pathol* **168**, 1107–1118.

Lim JO, Huh JS, Abdi SIH, Ng SM & Yoo JJ (2015). Functionalized biomaterials—oxygen releasing scaffolds. *J Biotechnol Biomater* **5**, 1.

Liu KJ, Gast P, Moussavi M, Norby SW, Vahidi N, Walczak T, Wu M & Swartz HM (1993). Lithium phthalocyanine: A probe for electron paramagnetic resonance oximetry in viable biological systems. *Proc Natl Acad Sci U S A* **90**, 5438–5442.

Longmuir IS (1981). Channels of oxygen transport from blood to mitochondria. *Adv Physiol Sci* **25**, 19–22.

Longmuir IS, Knopp JA, Benson D & Gregson H (1981). Intracellular microheterogeneity of oxygen concentrations. *Adv Physiol Sci* **25**, 43.

Maeda S, Nakagawa S, Suga M, Yamashita E, Oshima A, Fujiyoshi Y & Tsukihara T (2009). Structure of the connexin 26 gap junction channel at 3.5Å resolution. *Nature* **458**, 597–602.

Menchaca HJ, Michalek VN, Rohde TD, O'Dea TJ & Buchwald H (1998). Decreased blood oxygen diffusion in hyper-cholesterolemia. *Surgery* **124**, 692–698.

Michiels C, Tellier C & Feron O (2016). Cycling hypoxia: A key feature of the tumor microenvironment. *Biochim Biophys Acta* **1866**, 76–86.

Missner A & Pohl P (2009). 110 Years of the Meyer-Overton rule: Predicting membrane permeability of gases and other small compounds. *Chem Phys Chem* **10**, 1405–1414.

Moeendarbary E, Valon L, Fritzsche M, Harris AR, Moulding DA, Thrasher AJ, Stride E, Mahadevan L & Charras GT (2013). The cytoplasm of living cells behaves as a poroelastic material. *Nat Mater* **12**, 253–261.

Möller M, Botti H, Batthyany C, Rubbo H, Radi R & Denicola A (2005). Direct measurement of nitric oxide and oxygen partitioning into liposomes and low density lipoprotein. *J Biol Chem* **280**, 8850–8854.

Möller MN & Denicola A (2018). Diffusion of nitric oxide and oxygen in lipoproteins and membranes studied by pyrene fluorescence quenching. *Free Radic Biol Med* **128**, 137–143.

Möller MN, Li Q, Chinnaraj M, Cheung HC, Lancaster JR & Denicola A (2016). Solubility and diffusion of oxygen in phospholipid membranes. *Biochim Biophys Acta* **1858**, 2923–2930.

Multhoff G & Vaupel P (2012). Radiation-induced changes in microcirculation and interstitial fluid pressure affecting the delivery of macromolecules and nanotherapeutics to tumors. *Front Oncol* **2**, 165.

Murphy CS, Liaw L & Reagan MR (2019). In vitro tissue-engineered adipose constructs for modelling disease. *BMC Biomed Eng* **1**, 27.

Olmeda B, Villén L, Cruz A, Orellana G & Perez-Gil J (2010). Pulmonary surfactant layers accelerate O_2 diffusion through the air-water interface. *Biochim Biophys Acta* **1798**, 1281–1284.

Pias SC (2020). Pathways of oxygen diffusion in cells and tissues: Hydrophobic channelling via networked lipids. *Adv Exp Med Biol*, **1232** 183–190.

Place TL, Domann FE & Case AJ (2017). Limitations of oxygen delivery to cells in culture: An underappreciated problem in basic and translational research. *Free Radic Biol Med* **113**, 311–322.

Plesnar E, Szczelina R, Subczynski WK & Pasenkiewicz-Gierula M (2018). Is the cholesterol bilayer domain a barrier to oxygen transport into the eye lens? *Biochim Biophys Acta* **1860**, 434–441.

Pohl P, Saparov SM & Antonenko YN (1998). The size of the unstirred layer as a function of the solute diffusion coefficient. *Biophys J* **75**, 1403–1409.

Polnaszek CF, Schreier S, Butler KW & Smith ICP (1978). Analysis of the factors determining the EPR spectra of spin probes that partition between aqueous and lipid phases. *J Am Chem Soc* **100**, 8223–8232.

Raguz M, Mainali L, Widomska J & Subczynski WK (2011). Using spin-label electron paramagnetic resonance (EPR) to discriminate and characterize the cholesterol bilayer domain. *Chem Phys Lipids* **164**, 819–829.

Richardson SL, Hulikova A, Proven M, Hipkiss R, Akanni M, Roy NBA & Swietach P (2020). Single-cell O_2 exchange imaging shows that cytoplasmic diffusion is a dominant barrier to efficient gas transport in red blood cells. *Proc Natl Acad Sci U S A* **117**, 10067–10078.

Ruan K, Song G & Ouyang G (2009). Role of hypoxia in the hallmarks of human cancer. *J Cell Biochem* **107**, 1053–1062.

Shen J, Khan N, Lewis LD, Armand R, Grinberg O, Demidenko E & Swartz H (2003). Oxygen consumption rates and oxygen concentration in molt-4 cells and their mtDNA depleted (ρ0) mutants. *Biophys J* **84**, 1291–1298.

Sidell BD (1998). Intracellular oxygen diffusion: The roles of myoglobin and lipid at cold body temperature. *J Exp Biol* **201**, 1119–1128.

Skulachev VP (1990). Power transmission along biological membranes. *J Membr Biol* **114**, 97–112.

Subczynski WK, Hyde JS & Kusumi A (1991). Effect of alkyl chain unsaturation and cholesterol intercalation on oxygen transport in membranes: A pulse ESR spin labelling study. *Biochemistry* **30**, 8578–8590.

Subczynski WK, Pasenkiewicz-Gierula M, McElhaney RN, Hyde JS & Kusumi A (2003). Molecular dynamics of 1-palmitoyl-2-oleoylphosphatidylcholine membranes containing transmembrane α-helical peptides with alternating leucine and alanine residues. *Biochemistry* **42**, 3939–3948.

Swartz HM (1973). Toxic oxygen effects. *Int Rev Cytol* **35**, 321–343.

Vaupel P (1976). Effect of percentual water content in tissues and liquids on the diffusion coefficients of O_2, CO_2, N_2, and H_2. *Pflügers Archiv* **361**, 201–204.

Vaupel P (2004). Tumor microenvironmental physiology and its implications for radiation oncology. *Semin Radiat Oncol* **14**, 198–206.

Vaupel P & Mayer A (2007). Hypoxia in cancer: Significance and impact on clinical outcome. *Cancer Metastasis Rev* **26**, 225–239.

Volkmer E, Drosse I, Otto S, Stangelmayer A, Stengele M, Kallukalam BC, Mutschler W & Schieker M (2008). Hypoxia in static and dynamic 3D culture systems for tissue engineering of bone. *Tissue Eng Part A*, **14**, 1331–1340.

Wang Q, Dotson RJ, Angles G & Pias SC (2020). Simulation study of breast cancer lipid changes affecting membrane oxygen permeability: Effects of chain length and cholesterol. *Adv Exp Med Biol* **1269**, (in press).

Weiner MD & Feigenson GW (2018). Presence and role of midplane cholesterol in lipid bilayers containing registered or antiregistered phase domains. *J Phys Chem B* **122**, 8193–8200.

Widomska J, Raguz M, Dillon J, Gaillard ER & Subczynski WK (2007*a*). Physical properties of the lipid bilayer membrane made of calf lens lipids: EPR spin labelling studies. *Biochim Biophys Acta* **1768**, 1454–1465.

Widomska J, Raguz M & Subczynski WK (2007*b*). Oxygen permeability of the lipid bilayer membrane made of calf lens lipids. *Biochim Biophys Acta* **1768**, 2635–2645.

Wittenberg BA & Wittenberg JB (1989). Transport of oxygen in muscle. *Annu Rev Physiol* **51**, 857–878.

Yokobori S, Nakae R, Yokota H, Spurlock MS, Mondello S, Gajavelli S & Bullock RM (2018). Subdural hematoma decompression model: A model of traumatic brain injury with ischemic-reperfusional pathophysiology: A review of the literature. *Behav Brain Res* **340**, 23–28.

Zander R (1975). Die Verteilung von physikalisch gelöstem Sauerstoff im extra und intrazellulären Kompartiment des menschlichen Organismus. PhD Thesis, Mainz.

Zander R (1976). Cellular oxygen concentration. *Adv Exp Med Biol* **75**, 463–467.

Zhou Y & MacKinnon R (2003). The occupancy of ions in the K^+ selectivity filter: Charge balance and coupling of ion binding to a protein conformational change underlie high conduction rates. *J Mol Biol* **333**, 965–975.

Zocher F, van der Spoel D, Pohl P and Hub JS (2013). Local partition coefficients govern solute permeability of cholesterol-containing membranes. *Biophys J* **105**, 2760–2770.

Additional information

Data availability statement

Data sharing is not applicable to this article, as all relevant data are included in the body of the paper.

Competing interests

The author declares that there are no conflicts of interest.

Author contributions

Sole author.

Funding

This work was funded by a gift from the Glendorn Foundation and by institutional funds of the New Mexico Institute of Mining and Technology.

Acknowledgements

The author thanks Peter Pohl for critically reading the manuscript, Richard Pastor and Joseph LaManna for helpful discussions, and Rachel Dotson for assistance with manuscript figure preparation and editing.

Keywords

hypoxia, molecular dynamics simulation, permeability, P_{O2} gradient, radiotherapy, tissue engineering